

New Phase Induced by Pressure in the Iron-Arsenide Superconductor $\text{Ba}_{1-x}\text{K}_x\text{Fe}_2\text{As}_2$

E. Hassinger,^{1,*} G. Gredat,¹ F. Valade,¹ S. René de Cotret,¹ A. Juneau-Fecteau,¹ J.-Ph. Reid,¹ H. Kim,²
M. A. Tanatar,² R. Prozorov,^{2,3} B. Shen,⁴ H.-H. Wen,^{4,5} N. Doiron-Leyraud,¹ and Louis Taillefer^{1,5,†}

¹*Département de physique & RQMP, Université de Sherbrooke, Sherbrooke, Québec, Canada J1K 2R1*

²*Ames Laboratory, Ames, Iowa 50011, USA*

³*Department of Physics and Astronomy, Iowa State University, Ames, Iowa 50011, USA*

⁴*Center for Superconducting Physics and Materials,*

National Laboratory of Solid State Microstructures and Department of Physics, Nanjing University, Nanjing 210093, China

⁵*Canadian Institute for Advanced Research, Toronto, Ontario, Canada M5G 1Z8*

(Dated: August 17, 2018)

The electrical resistivity ρ of the iron-arsenide superconductor $\text{Ba}_{1-x}\text{K}_x\text{Fe}_2\text{As}_2$ was measured in applied pressures up to 2.6 GPa for four underdoped samples, with $x \simeq 0.16, 0.18, 0.19$ and 0.21 . The antiferromagnetic ordering temperature T_N , detected as a sharp anomaly in $\rho(T)$, decreases linearly with pressure. At pressures above $P \simeq 1.0$ GPa, a second sharp anomaly is detected at a lower temperature T_0 , which rises with pressure. We attribute this second anomaly to the onset of a phase that causes a reconstruction of the Fermi surface. This new phase expands with increasing x and it competes with superconductivity. We discuss the possibility that a second spin-density wave orders at T_0 , with a \mathbf{Q} vector distinct from that of the spin-density wave that sets in at T_N .

PACS numbers: 74.25.Fy, 74.70.Dd

Superconductivity often appears on the border of antiferromagnetic order,¹ as in organic conductors,² heavy-fermion compounds,³ and electron-doped cuprates.⁴ Tuning the system with applied pressure or chemical substitution causes the antiferromagnetic ordering temperature T_N to fall and a superconducting phase to eventually appear, with the superconducting transition temperature T_c rising until the quantum critical point where T_N goes to zero, and falling thereafter to form a dome-like region of superconductivity in the phase diagram. In cuprates, hole doping has the additional effect of inducing the onset of a second phase, with stripe order⁵ – a unidirectional modulation of the spin and charge densities. This stripe order competes with superconductivity, and so causes a dip in T_c where it peaks. Antiferromagnetism and stripe order cause a reconstruction of the Fermi surface, detected for example in measurements of quantum oscillations and transport properties (*e.g.* resistivity, Hall and Seebeck coefficients).^{6,7}

In the iron arsenide BaFe_2As_2 , substitution of K for Ba, Co or Ru for Fe, and P for As all produce the same type of phase diagram, whereby T_N falls and a T_c dome surrounds the quantum critical point where $T_N \rightarrow 0$.⁸ The application of pressure to BaFe_2As_2 produces a similar phase diagram.⁹ The antiferromagnetic order is unidirectional, with wavevector $\mathbf{Q} = (\pi, 0)$ (or $\mathbf{Q} = (0, \pi)$). It causes the lattice to undergo a transition from tetragonal at high temperature to orthorhombic at low temperature. The structural transition is either simultaneous with T_N or slightly before it, as in K-doped¹⁰ or Co-doped BaFe_2As_2 ,¹¹ respectively. In Co-doped and K-doped BaFe_2As_2 , Fermi-surface reconstruction causes a distinct change in the electrical resistivity $\rho(T)$ below T_N .^{8,12}

In this Article, we report a study of the pressure-temperature phase diagram of $\text{Ba}_{1-x}\text{K}_x\text{Fe}_2\text{As}_2$ at K concentrations ranging from $x \simeq 0.16$ to $x \simeq 0.21$. We find that a pressure in excess of ~ 1.0 GPa induces the onset of a new phase whose extent in the phase diagram increases with x , and whose emergence causes a suppression of superconductivity. While the underlying order has yet to be determined, we discuss the possibility of two successive spin-density waves, the first setting in at T_N and the second at T_0 , with $\mathbf{Q} = (\pi, 0)$ and $\mathbf{Q} = (0, \pi)$ (or vice-versa), respectively.

Methods.– Single crystals of $\text{Ba}_{1-x}\text{K}_x\text{Fe}_2\text{As}_2$ were grown from self flux.¹³ Four underdoped samples were measured, with a superconducting transition temperature $T_c = 7.3 \pm 0.5$ K, 10.5 ± 0.5 K, 15.0 ± 0.5 K and 18.0 ± 0.5 K, respectively. Using the relation between T_c and the nominal K concentration x reported in ref. 10, we obtain $x = 0.161, 0.175, 0.194$ and 0.207 , respectively. For simplicity, we label these $x = 0.16, 0.18, 0.19$ and 0.21 . These x values are also consistent with the measured antiferromagnetic ordering temperature T_N (which coincides with the structural transition from tetragonal to orthorhombic),¹⁰ equal to 115 ± 1 K, 111 ± 1 K, 105 ± 1 K and 98 ± 1 K, respectively. Hydrostatic pressures up to 2.63 GPa were applied with a hybrid piston-cylinder cell,¹⁴ using a 50:50 mixture of n-pentane:isopentane.¹⁵ The pressure was measured via the superconducting transition of a lead wire inside the pressure cell. The electrical resistivity ρ was measured for a current in the basal plane of the orthorhombic crystal structure, with a standard four-point technique using a Lakeshore ac-resistance bridge. When a magnetic field was applied, it was along the c axis, normal to the basal plane. The transition temperatures are defined as follows: T_c is where $\rho = 0$; T_N and T_0 are extrema in the derivative $d\rho/dT$ (Fig. 1).

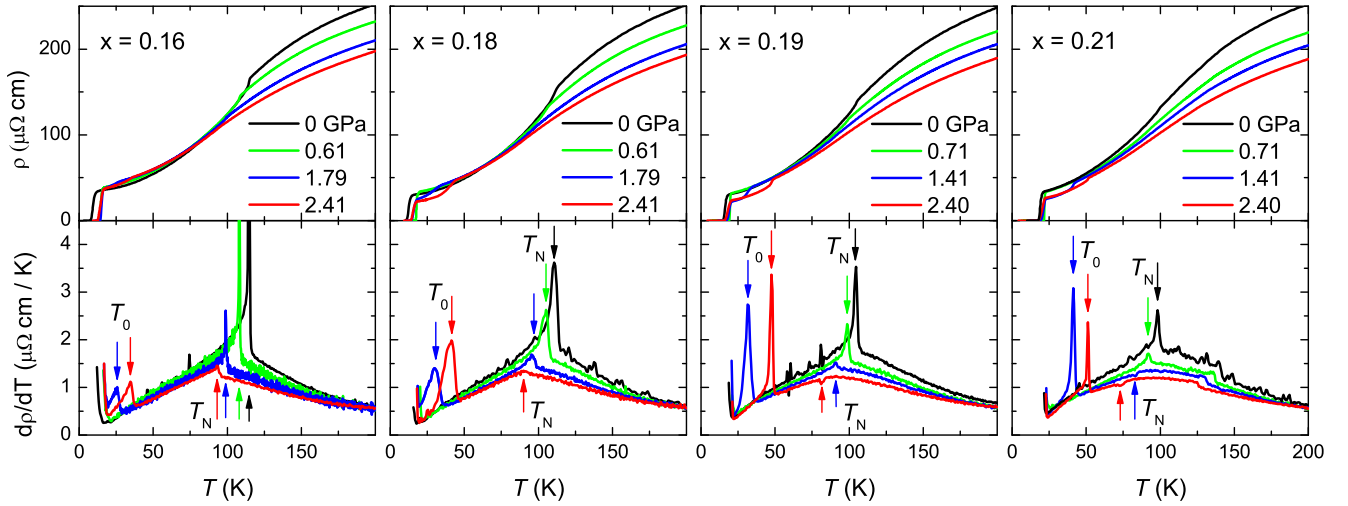


FIG. 1: *Top*: In-plane electrical resistivity of $\text{Ba}_{1-x}\text{K}_x\text{Fe}_2\text{As}_2$ with $x = 0.16$, $x = 0.18$, $x = 0.19$ and $x = 0.21$ (different columns) for different pressures, as indicated. *Bottom*: Temperature derivative of the data in the top panels. The peak (dip) near 100 K signals the onset of antiferromagnetic order at T_N . The peak at lower temperature, seen for $P > 1.0$ GPa, signals the onset of a second phase at T_0 .

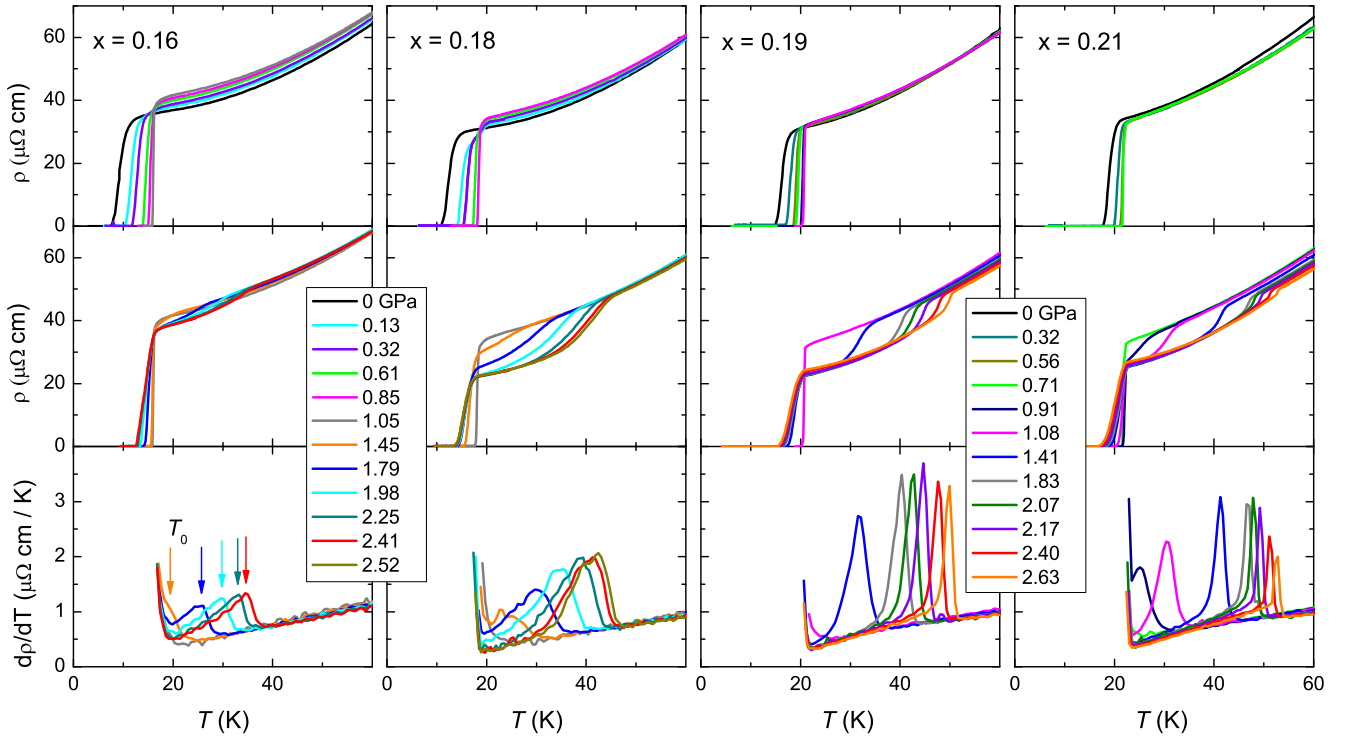


FIG. 2: *Top and middle*: Resistivity of $\text{Ba}_{1-x}\text{K}_x\text{Fe}_2\text{As}_2$ with $x = 0.16$, $x = 0.18$, $x = 0.19$ and $x = 0.21$ (different columns) below 60 K, for pressures as indicated. *Bottom*: Temperature derivative of the curves in the middle panel. The arrows mark the anomaly at T_0 .

Resistivity.— In Fig. 1, the resistivity of $\text{Ba}_{1-x}\text{K}_x\text{Fe}_2\text{As}_2$ is plotted as a function of temperature, at four representative pressures for $x = 0.16$, 0.18, 0.19 and 0.21. To remove uncertainties coming from the geometric factors of the different samples, we set $\rho = 300 \mu\Omega$ cm at $T = 300$ K, in agreement with

previous studies.¹² The antiferromagnetic transition at T_N is detected as a sharp peak in the derivative $d\rho/dT$, which becomes less and less pronounced with pressure. For $x = 0.19$ and $x = 0.21$, the anomaly changes from a peak to a dip, above $P = 1.83$ GPa and $P = 1.08$ GPa, respectively. The same effect is observed with increasing

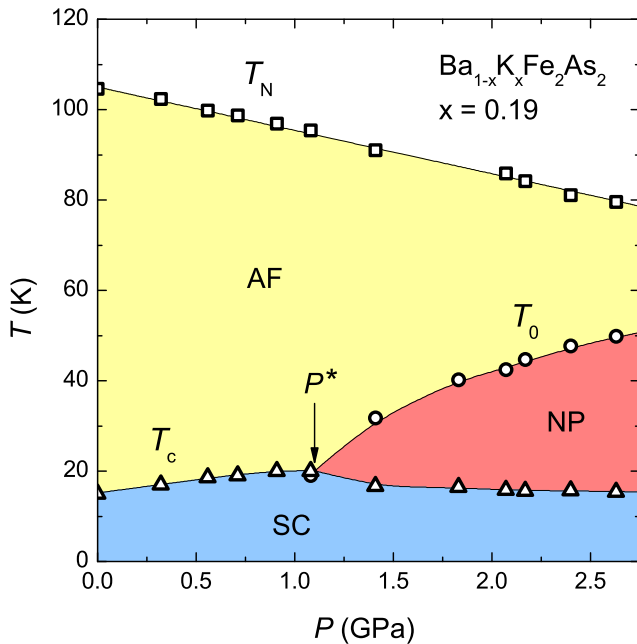


FIG. 3: Pressure-temperature phase diagram of $\text{Ba}_{1-x}\text{K}_x\text{Fe}_2\text{As}_2$ for $x = 0.19$, showing the antiferromagnetic (AF) ordering temperature T_N , the superconducting (SC) transition temperature T_c and the anomaly at T_0 , as a function of pressure. Error bars are smaller than the size of the symbols. We attribute the anomaly at T_0 to the onset of a new phase (NP), whose order has yet to be determined. P^* is the critical pressure above which the new phase is present.

x at ambient pressure.¹² This change seems to happen when T_N falls below ~ 87 K.

Above T_N , ρ decreases with pressure, at the rate of $-10\%/GPa$ at 200 K. Below T_N , the pressure dependence of ρ has nearly vanished and $\rho = \rho_0 + AT^n$, with $n = 2$ for $x = 0.16$ and 0.18 , $n = 1.85 \pm 0.05$ for $x = 0.19$ and 0.21 , in agreement with $n = 1.90$ at $x = 0.20$ reported previously.¹² n is independent of pressure and A decreases only slightly with pressure. The drop in $\rho(T)$ below T_N is due to the reconstruction of the Fermi surface caused by the antiferromagnetic order, where the loss in carrier density is more than compensated by the reduction in scattering, as in stoichiometric BaFe_2As_2 .¹²

For $P > 1$ GPa, a second drop in $\rho(T)$ is observed at lower temperature. It produces a peak in $d\rho/dT$ similar to that at T_N , revealing the onset of a second Fermi-surface reconstruction, at a temperature labelled T_0 . In Fig. 2, a zoom at low temperature shows that T_0 moves up under pressure, in contrast to T_N which moves down.

The superconducting transition moves up with pressure initially, and it becomes sharper where T_c is maximal. At pressures where the new phase is present, T_c moves down with pressure and the transition widens. At $P > 1$ GPa, the onset of the superconducting drop is independent of pressure.

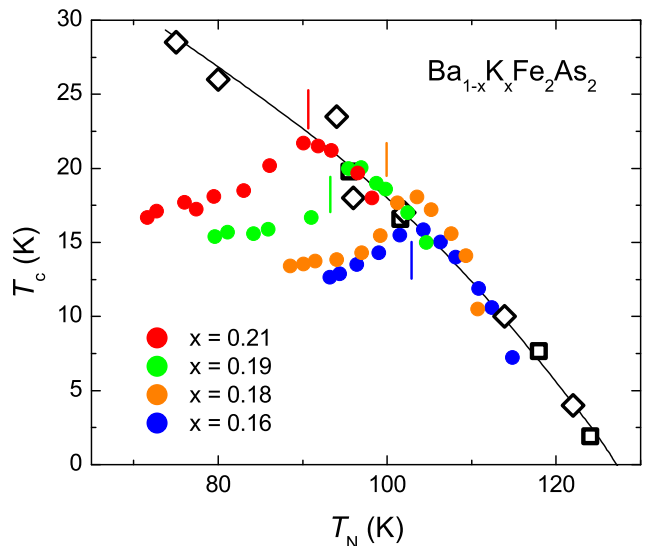


FIG. 4: Evolution of the superconducting temperature T_c of underdoped $\text{Ba}_{1-x}\text{K}_x\text{Fe}_2\text{As}_2$ as a function of the corresponding antiferromagnetic temperature T_N , obtained by varying either x at ambient pressure (open black symbols) or pressure at fixed x , for 4 values of x , as indicated. The data come from neutron (open diamonds, ref. 10) and transport (open squares, ref. 12) measurements. The line is a guide to the eye. The small vertical lines indicate the position of P^* . Note that pressure and doping have the same effect in both decreasing T_N and increasing T_c , until pressure induces the onset of a new phase at P^* , whereupon T_c drops from its otherwise monotonic increase vs P and x .

Phase diagram.— In Fig. 3, the evolution of T_N , T_0 and T_c with pressure is displayed on a phase diagram for $x = 0.19$. Initially, T_c rises as T_N falls, reflecting the competition between antiferromagnetic and superconducting phases. At low pressure, the pressure-tuned competition mimics the well-known concentration-tuned competition (Fig. 4). T_c reaches a maximal value of 20.0 ± 0.2 K at $P \simeq 1$ GPa, and then it falls. The peak in T_c coincides with the point where the T_0 and T_c lines intersect; we label this pressure P^* . (The point $T_0 < T_c$ at 1.08 GPa was determined by the application of a magnetic field to lower T_c ; see Fig. 5.)

Qualitatively identical phase diagrams are obtained for all four samples (Fig. 6). With increasing x , the antiferromagnetic phase shrinks, while the new phase expands (to higher temperature and lower pressure). The peak in $T_c(P)$ correlates with the appearance of the new phase, i.e. it coincides with P^* . As shown in Fig. 7a, T_N decreases with doping the same way at zero pressure and at 2.4 GPa. At 2.4 GPa, T_0 increases linearly with doping, so that T_0 and T_N are expected to become equal at $x \simeq 0.23$. The maximum T_c attained under pressure, T_c^{max} , increases with x (Fig. 7b); at high x , it approaches the value of T_c at zero pressure since P^* moves down with x (Fig. 7c).

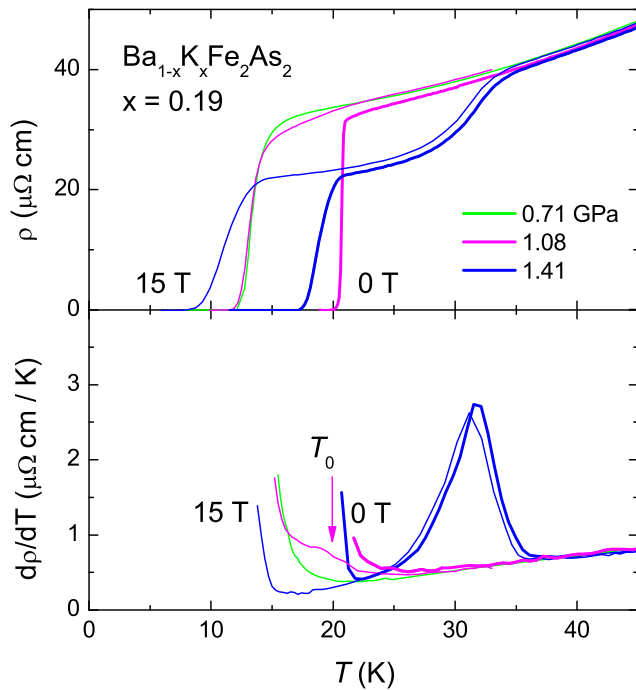


FIG. 5: *Top*: Resistivity of sample $x = 0.19$ as a function of temperature for pressures as indicated, at $H = 0$ T (thick lines) and $H = 15$ T (thin lines). *Bottom*: The temperature derivatives of the curves in the top panel. Note how the anomaly in the 1.08 GPa curve appears when the superconducting transition is lowered by the magnetic field, at T_0 (arrow).

Discussion.— A drop in the resistivity could have a number of possible origins. First, we rule out the possibility of an incomplete superconducting transition by studying the effect of a magnetic field. In Fig. 5, $\rho(T)$ for $x = 0.19$ is shown at $H = 0$ and $H = 15$ T. While T_c shifts down by ~ 7 K, T_0 is only suppressed by about 0.7 K. A second possibility is a Lifshitz transition. Within a single antiferromagnetic phase, the Fermi surface can undergo a second reconstruction below the original one at T_N when the spin-density-wave order parameter exceeds a certain critical value. However, such a Lifshitz transition is unlikely to be the explanation here, as T_0 and T_N respond in opposite directions to both pressure (Fig. 6) and K concentration (Fig. 7).

Instead, the phenomenology strongly suggests that a second phase transition occurs at T_0 , to a new phase with currently unknown order. Let us mention two possible density-wave scenarios. The first is a charge-density wave. ARPES data on BaFe_2As_2 has revealed highly parallel sections of the Fermi surface inside the antiferromagnetic phase.¹⁶ Such features suggest the possibility of an incommensurate charge-density-wave instability favored by the good nesting conditions, which may be improved by tuning x and applying pressure.

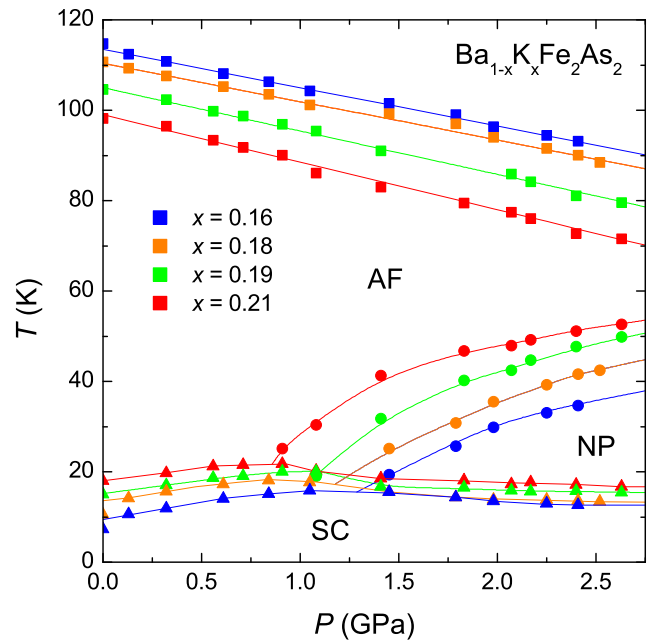


FIG. 6: Phase diagram as in Fig. 3, for all four concentrations x , as indicated by color-coded symbols.

A second possibility is that T_N and T_0 are the onset temperatures of two successive spin-density-wave phases. The situation is reminiscent of the two successive charge-density-wave transitions in the rare-earth tri-tellurides $R\text{Te}_3$,¹⁷ where nesting at a wavevector \mathbf{Q}_1 gaps out part of the Fermi surface below the first transition, at T_{c1} , and nesting at a wavevector \mathbf{Q}_2 , perpendicular to \mathbf{Q}_1 , further gaps out the Fermi surface below the second transition, at $T_{c2} < T_{c1}$. By changing the rare-earth ion R from Dy to Tm, the two transition temperatures go in opposite directions: T_{c1} drops while T_{c2} rises.¹⁷ This is interpreted as follows: as the first gap, Δ_1 , decreases, more of the Fermi surface remains after reconstruction below T_{c1} and so more of it can take part in the nesting at \mathbf{Q}_2 , thus producing a stronger gap Δ_2 , and hence a larger T_{c2} .¹⁷

The fact that T_N and T_0 go in opposite directions with pressure in $\text{Ba}_{1-x}\text{K}_x\text{Fe}_2\text{As}_2$ suggests a similar picture. The first spin-density wave orders below T_N with $\mathbf{Q}_1 = (\pi, 0)$ (within a given orthorhombic domain), causing two of the four electron pockets in the Fermi surface to reconstruct. The proposed scenario is that a second spin-density wave orders below T_0 , with a different wave vector, \mathbf{Q}_2 . It is conceivable that $\mathbf{Q}_2 \simeq (0, \pi)$, causing the other two electron pockets to reconstruct.

Three other features of our data appear consistent with a scenario of two related spin-density-wave phases. First, the two transitions, at T_N and T_0 , cause similar changes in the resistivity: $\rho(T)$ drops in both cases, and the drop is of comparable sharpness (see $d\rho/dT$ in Fig. 1). Secondly, with increasing doping or pressure, the anomaly in $d\rho/dT$ becomes weaker at T_N but stronger at T_0 . This is consistent with nesting conditions that deteriorate at

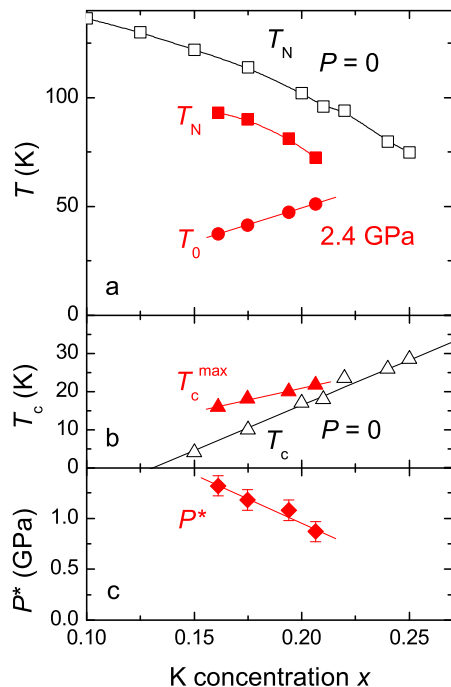


FIG. 7: Evolution of various properties of $\text{Ba}_{1-x}\text{K}_x\text{Fe}_2\text{As}_2$ with K concentration x . a) Antiferromagnetic ordering temperature T_N at $P = 0$ (open black squares, from neutron scattering data¹⁰) and at $P = 2.4$ GPa (full red squares, from Fig. 6). Onset temperature T_0 for the new phase, at $P = 2.4$ GPa (full red circles, from Fig. 6). All lines are a guide to the eye. b) T_c at zero pressure (open triangles, from magnetization data¹⁰); the linear fit (line) is used to define the value of x in our samples. Also shown is the maximal value of T_c attained under pressure, labelled T_c^{max} (full triangles), with a linear fit (line). c) The pressure P^* where the new phase appears (diamonds); the line is a linear fit.

\mathbf{Q}_1 and improve at \mathbf{Q}_2 with increasing P or x . Finally, the new phase appears to compete with superconductivity, as does the antiferromagnetic order. Below P^* , T_c increases while T_N decreases with pressure. Above P^* , as the new phase grows, T_c drops and the dependence of T_c on T_N deviates (Fig. 4).

In summary, we report an anomaly in the temperature dependence of the resistivity of underdoped $\text{Ba}_{1-x}\text{K}_x\text{Fe}_2\text{As}_2$ for $P > 1$ GPa that signals the onset of a Fermi-surface reconstruction at a temperature T_0 below the antiferromagnetic temperature T_N . We attribute this reconstruction to a new phase that onsets below T_0 . Whether this phase involves order in the spin, charge or orbital degree of freedom remains to be determined. However, the overall phenomenology is consistent with a scenario of two related spin-density-wave phases setting in successively at T_N and T_0 , with wavevectors $\mathbf{Q}_1 \simeq (\pi, 0)$ and $\mathbf{Q}_2 \simeq (0, \pi)$, respectively.

We thank A. V. Chubukov, R. Fernandes, I. R. Fisher, S. A. Kivelson, J. Schmalian and R. Thomale for fruitful discussions and J. Corbin for his assistance with the experiments. The work at Sherbrooke was supported by a Canada Research Chair, CIFAR, NSERC, CFI and FQRNT. The work at the Ames Laboratory was supported by the DOE-Basic Energy Sciences under Contract No. DE-AC02-07CH11358. The work in China was supported by NSFC and the MOST of China (#2011CBA00100).

* Electronic address: elena.hassinger@usherbrooke.ca

† Electronic address: louis.taillefer@usherbrooke.ca

¹ P. Monthoux *et al.*, Nature **450**, 1177 (2007).

² N. Doiron-Leyraud *et al.*, Phys. Rev. B **80**, 214531 (2009).

³ G. Knebel *et al.*, C. R. Phys. **12**, 542 (2011).

⁴ K. Jin *et al.*, Nature **476**, 73 (2011).

⁵ N. Doiron-Leyraud and L. Taillefer, Physica C **481**, 161 (2012).

⁶ L. Taillefer, J. Phys.: Condens. Matter **21**, 164212 (2009).

⁷ L. Taillefer, Annu. Rev. Condens. Matter Phys. **1**, 51 (2010).

⁸ P. C. Canfield and S. L. Budk'o, Annu. Rev. Condens. Matter Phys. **1**, 27 (2010).

⁹ S. K. Kim *et al.*, Phys. Rev. B **84**, 134525 (2011).

¹⁰ S. Avci *et al.*, Phys. Rev. B **85**, 184507 (2012).

¹¹ D. K. Pratt *et al.*, Phys. Rev. Lett. **103**, 087001 (2009).

¹² B. Shen *et al.*, Phys. Rev. B **84**, 184512 (2011).

¹³ H.-Q. Luo *et al.*, Supercond. Sci. Technol. **21**, 125014 (2008).

¹⁴ I. R. Walker, Rev. Sci. Instrum. **70**, 3402 (1999).

¹⁵ W. J. Duncan *et al.*, J. Phys.: Condens. Matter **22**, 052201 (2010).

¹⁶ T. Kondo *et al.*, Phys. Rev. B **81**, 060507 (2010).

¹⁷ N. Ru *et al.*, Phys. Rev. B **77**, 035114 (2008).